Antenna Effect in BODIPY-(Zn)Porphyrin Entities Promotes H 2 Evolution in Dye-Sensitized Photocatalytic Systems

Vasilis Nikolaou, Georgios Charalambidis, Georgios Landrou, Emmanouil Nikoloudakis, Aurélien Planchat, Ronilnta Tsalameni, Karen Junghans, Axel Kahnt, Fabrice Odobel, Athanassios Coutsolelos

▶ **To cite this version:**

Vasilis Nikolaou, Georgios Charalambidis, Georgios Landrou, Emmanouil Nikoloudakis, Aurélien Planchat, et al.. Antenna Effect in BODIPY-(Zn)Porphyrin Entities Promotes H 2 Evolution in Dye-Sensitized Photocatalytic Systems. ACS Applied Energy Materials, 2021, 4 (9), pp.10042-10049. 10.1021/acsaem.1c01975 . hal-03421775

HAL Id: hal-03421775
https://hal.science/hal-03421775v1

Submitted on 9 Nov 2021

HAL is a multi-disciplinary open access archive for the deposit and dissemination of scientific research documents, whether they are published or not. The documents may come from teaching and research institutions in France or abroad, or from public or private research centers.

L'archive ouverte pluridisciplinaire **HAL**, est destinée au dépôt et à la diffusion de documents scientifiques de niveau recherche, publiés ou non, émanant des établissements d'enseignement et de recherche français ou étrangers, des laboratoires publics ou privés.

Antenna Effect in BODIPY-(Zn)Porphyrin entities Promotes H_2 Evolution in Dye-sensitized Photocatalytic Systems

Vasilis Nikolaou,[a]* *Georgios Charalambidis,*[a] *Georgios Landrou*[a], *Emmanouil Nikoloudakis,*[a] *Aurélien Planchat,*[b] *Ronilnta Tsalameni,*[a] *Karen Junghans,*[c] *Axel Kahnt,*[c]* *Fabrice Odobel,*[b]* *and Athanassios G. Coutsolelos*[a]*

[a] Laboratory of Bioinorganic Chemistry, Department of Chemistry, University of Crete, Voutes Campus, 70013 Heraklion, Crete, Greece.

[b] Université de Nantes, CNRS, Chimie et Interdisciplinarité: Synthèse, Analyse, Modélisation (CEISAM), UMR 6230, 2 rue de la Houssinière, 44322 Nantes cedex 3, France.

[c] Leibniz Institute of Surface Engineering (IOM), Permoserstr, 15, 04318 Leipzig, Germany.

* Corresponding authors: acoutsol@uoc.gr

fabrice.Odobel@univ-nantes.fr

axel.kahnt@iom-leipzig.de

v.nikolaou@uoc.gr

Abstract

In this study, we report the preparation of BODIPY-(Zn)Porphyrin hybrids and their utilization in photocatalytic H_2 production from water. These entities were employed as photosensitizers upon their chemisorption onto the surface of platinum-doped titanium dioxide nanoparticles ($PtTiO_2$) which acted as photocatalysts. We prepared two diverse BODIPY-(Zn)Porphyrin entities, in which the BODIPY moiety is either covalently attached (**BDP-Por**) or axially coordinated (**BDP(Im)-Por**) with the (Zn)Porphyrin; in order to evaluate the impact of the different connectivity between the chromophores in photocatalytic in H_2 evolution. Overall, we developed highly efficient dye-sensitized photocatalytic systems (DSPs) based on noble metal-free photosensitizers reaching 18,600 Turnover Numbers (TONs) and 225 mmol(H_2) $g(cat)^{-1}\,h^{-1}$.

Keywords: Antenna effect, Photo-catalytic Hydrogen Production, Dye-sensitized Photocatalytic Systems (DSPs), Porphyrin, BODIPY, Axial Coordination, Covalent attachment.

Introduction

Currently, the primary energy sources derive from the combustion of fossil fuels, namely natural gas, oil and coal.[1,2] As a result of their prolonged usage, vital issues affecting the sustainability of the planet have emerged in recent years, namely global warming and climate change due to production of green-house gases such as carbon dioxide.[3] Hence, it is imperative to utilize renewable and clean fuels aiming to establish a socially and economically sustainable future.[4] Solar energy is unquestionably one of the best candidate for that purpose since being abundant, clean and could meet future energy requirements.[5] Developing devices that efficiently exploit solar energy has dominated the scientific interest worldwide.[4,6] To that end, many scientific reports have been published over the years dealing with the direct conversion of sunlight into chemical energy.[7,8] Photocatalytic hydrogen (H_2) production from water (H_2O) is an auspicious approach since an abundant precursor can be converted into a useful fuel.[9,10] In this context, numerous photocatalytic systems have been developed over the years that are able to convert solar energy into H_2.[11-13]

In 1972, Honda and Fujishima introduced a novel approach towards photocatalytic H_2 production using semiconductor materials.[14] Titanium dioxide (TiO_2) is the most widely used semiconductor in light-driven H_2 evolution due its distinctive features. More specifically, TiO_2 is non-toxic of low cost and retains great photo-stability.[15-17] However, TiO_2 absorbs only in the UV part of the absorption spectrum, has a wide band gap (3.2-3.3 eV) and also undergoes fast electron-hole recombination. Due to all the above drawbacks, TiO_2 exhibits limited photocatalytic performance towards H_2 production.[18] Nevertheless, dye sensitization of TiO_2 with the appropriate chromophores can efficiently shift absorption towards the visible light

region.[19] Over the last years, various research groups have reported different approaches, in which dye-sensitized TiO_2 nanoparticles (NPs) were utilized for efficient photocatalytic hydrogen generation.[20-22] The most common one is the attachment of one sensitizer onto platinum-doped titanium dioxide nanoparticles ($PtTiO_2$ NPs).[23] This approach is usually referred as dye-sensitized photocatalytic systems (DSPs) and was initially established by Shimitzu and coworkers[24] and also studied by Abe et al.[25] More recently, Reisner and coworkers have further developed the concept of DSPs for H_2 evolution.[23,26] Although there are many examples of DSPs in the literature, the majority of these reports is based on a single sensitizer as unique light absorber. Interestingly, only a few recent research works describe the utilization of dyadic systems consisting of different chromophore units.[27-30] In particular, Eisenberg, McCamant and coworkers in 2018 illustrated that a rhodamine-platinum diimine dithiolate complex dyad was a very efficient photosensitizer (PS) towards H_2 production reaching 70,700 turnover numbers (TONs).[27] The same year, Sun *et al.* reported the synthesis and the H_2 evolution studies of a chlorophyll-indoline dyad which exhibited a maximum TON of 1,044.[30] In addition, Ho *et al.* illustrated that a covalently connected BODIPY-(Zn)Porphyrin dye exhibits 12,800 TONs over 120 hours of illumination.[28] It is worth mentioning that multichromophoric systems have also been reported in order to effectively enhance the photovoltaic performance in dye-sensitized solar cells (DSSCs).[31,32] Porphyrin-BODIPY dyads have been thoroughly examined as sensitizers in DSSCs due to the antenna effect between the chromophores and also because of their complementary absorption features.[33-37] In stark contrast, there is only one example of a Porphyrin-BODIPY dyad in DSPs for H_2 evolution.[28] However, plenty aspects that could impact H_2 evolution are still not studied in such Porphyrin-BODIPY systems. Namely, the type of connection between

the two entities or the supplementary antenna effect by the addition of an extra BODIPY.

Herein, we demonstrate the development of DSPs for H_2 evolution using BODIPY-(Zn)Porphyrin entities chemisorbed onto $PtTiO_2$ NPs. We utilized BODIPY moieties (BDP) as extra light harvesters to (Zn)Porphyrin in order to amplify light capture by exploiting the antenna effect. We explored the impact of the diverse connection between the BODIPY and the porphyrin chromophore to the photocatalytic efficiency of the DSPs and compared the covalent attachment of BODIPY (**BDP-Por**) *versus* the axial coordination (**BDP(Im)-Por**) with a (Zn)porphyrin (**Figure 1**). Furthermore, an additional BODIPY unit was axially coordinated onto the covalent **BDP-Por** dyad with the purpose of increasing the photocatalytic activity through the supplementary antenna effect (**BDP-Por-BDP(Im)**, **Figure 1**). We have also synthesized the reference chromophores of the dyads, namely the BODIPY (**BDP**), the (Zn)Porphyrin (**Por**) and the **BDP(Im)**. Overall, **BDP-Por** and **BDP(Im)-Por** reached 17,500 and 13,700 TONs (*vs* PS), respectively, whereas **BDP-Por-BDP(Im)** (18,600 TONs) exhibited a record high H_2 production of 225 mmol(H_2) g(cat)$^{-1}$ h^{-1} with respect to similar noble metal free photosensitizers in the literature.[30,38-46]

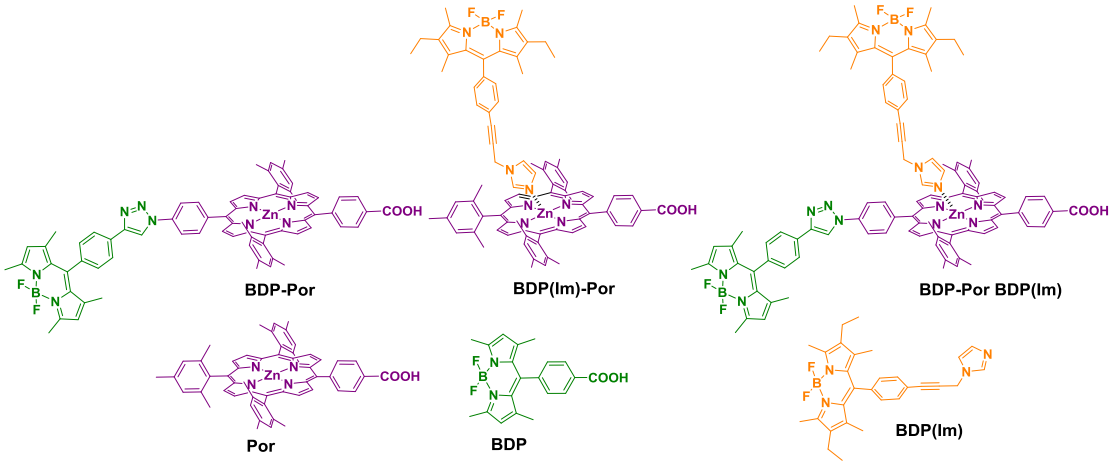

Figure 1. Molecular structures of the entities investigated in this study: **BDP-Por**, **BDP(Im)-Por** , **BDP-Por-BDP(Im)** and the reference dyes **BDP**, **Por** and **BDP(Im)**.

Results and discussion

Molecular design and characterization.

BDP-Por dyad, **BDP** and **BDP(Im)** were prepared and characterized according to published experimental approaches previously reported by our research group.[34,47,48] **Por** was synthesized using straightforward synthetic procedures as described in the experimental section of this work (ESI). The synthetic approach followed for the preparation of **Por** is illustrated in **Scheme S1** and the ^{1}H NMR spectra of the intermediate and final compound are provided in **Figures S1-S4**. In detail, the first step for the synthesis of **Por** was the metalation of **TMP(COOMe)**[49] with zinc; using CH_2Cl_2, MeOH and $Zn(OAc)_2x2H_2O$. Subsequently, a hydrolysis reaction took place in order to convert the ester group of **Zn-TMP(COOMe)** into an acid, yielding the desired Zn-TMP(COOH) **(Por)**.

Photophysical investigation.

To shed light on the photophysical features of the **BDP-Por** dyad, absorption and fluorescence measurements were performed. As expected, the absorption spectrum of **BDP-Por** dyad (**Figure S5**) is the superimposition of the UV-Vis spectra of its components.[50] More specifically, a Soret band at 426 nm, two Q-bands at 557 and 598 nm along with a sharp band at 501 nm can be detected.

The absorption spectra of these dyes were also recorded on thin TiO_2 films (**Figure S6**). On TiO_2 films, the absorption below 450 nm is not informative as the intensity of the Soret band is too high to give reliable values. This is in agreement with previous studies.[51-54] These spectra are, however, informative as they show that: i) **BDP(Im)** binds to TiO_2 surface, most certainly by H-bonding between imidazole

and the proton of TiO_2, ii) **BDP(Im)** exhibits a bathochromically shifted absorption band relative to that of BODIPY in **BPD-Por** due to the extended π-conjugation promoted by the triple bond, iii) the connection of BODIPY with zinc porphyrin *via* covalent attachment or by axial coordination increases the light absorption between 450-550 nm, where zinc porphyrin has small absorption coefficient; iv) the dyad **BPD-Por** also takes advantage of the presence of **BDP(Im)** as supplementary antenna; because the two BODIPYs have different absorption spectra (see point (ii) above) and finally v) the axial binding of imidazole unit of **BDP(Im)** on the zinc porphyrin is clearly witnessed by the red shift of its Q bands of ZnP in **BDP(Im)-Por** and **BDP-Por-BDP(Im)**.[32,55]

The steady-state fluorescence and excitation spectra recorded in solution reveal that energy transfer process occurs from **BDP** to **Por** in the **BDP-Por** dyad **(Figure 2a)**. In particular, **BDP** exhibits an intense fluorescence band centered at 515 nm, which is almost quantitatively quenched (94%) in the **BDP-Por** dyad (λ_{exc} = 490 nm). In addition, selective excitation of the BDP entity in **BDP-Por** dyad, leads to the appearance of the two emission bands (at 607 and 655 nm) that can undoubtedly assigned to Zn-Porphyrin-based fluorescence. Finally, energy transfer in the **BDP-Por** dyad is supported by its excitation spectrum, which matches with its absorption spectrum featuring the characteristic absorption band of BODIPY chromophore around 500 nm (**Figure 2b**). The incorrect matching on the Soret band (around 430 nm) is due to the too high absorbance (> 0.5) on this transition inherent of its high extinction coefficient. Overall, all the experiments indicate an almost quantitative energy transfer from BODIPY to porphyrin and are in agreement with previous works in witch similar chromophores have been utilized.[32,33,56-59] For transient absorption

studies comparing the charge charier properties of $PtTiO_2$ NPs with TiO_2 NPs see supporting information.

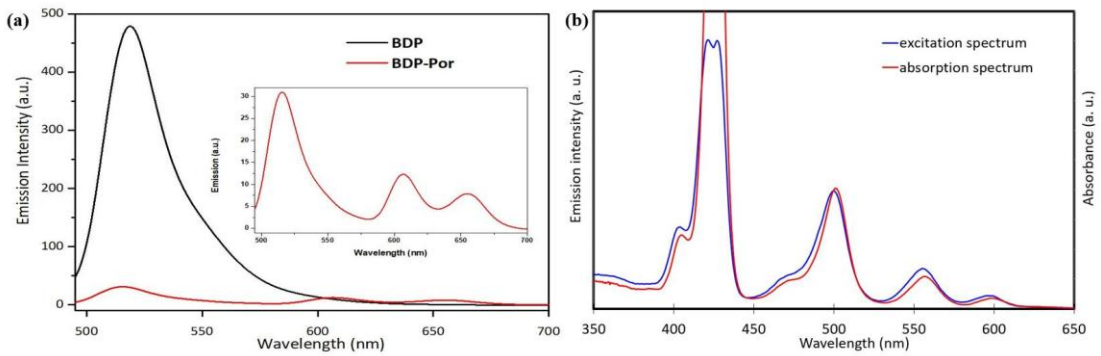

Figure 2. (a) Emission spectra of **BDP** (black) and **BDP-Por** dyad (red) upon excitation at 490 nm. **(b)** Absorption (red) and excitation (blue) spectrum of **BDP-Por** dyad recorded in dichloromethane when monitoring the emission at 660 nm.

Photo-induced H_2 production experiments.

The initial step of the photocatalytic measurements was the chemisorption of the sensitizers onto the $PtTiO_2$ NPs (see experimental section for details). In all the photocatalytic experiments we utilized dye-sensitized Pt-TiO_2 NPs in aqueous solution which contained 1.0 M of Ascorbic Acid (AA) as sacrificial electron donor (SED), at pH=4. In **Figure 3a** the H_2 production plots (in TONs *vs* PS) of **BDP**, **Por**, **BDP-Por** dyad and **Por/BDP** (1:1 mixture) are illustrated. The TONs were 470 and 980 for **BDP** and **Por** respectively. Whereas, **BDP/Por** (1:1 mixture) exhibited 860 TONs. Interestingly, **BDP-Por** dyad reached 1,700 TONs upon 120 h of continuous light irradiation demonstrating that is more efficient compared to either the chromophore counterparts (**BDP** and **Por**) or the 1:1 mixture of **BDP/Por**. Thus, **BDP-Por** dyad outperformed both the monomers as well as their combination; showing that the antenna effect due to the covalent attachment of the BDP onto the (Zn)Porphyrin is beneficial towards H_2 evolution.

With the purpose of optimizing the catalytic activity of **BDP-Por**, we used different amounts of the dyad by either increasing or reducing the final mole of **BDP-Por** in the photocatalytic experiments. By decreasing the amount of **BDP-Por** from $4.15x10^{-7}$ to $7.0x10^{-8}$ mole the TONs were increased from 640 to 2,500. Further decrease of **BDP-Por** to $2.3x10^{-8}$ and $1.0x10^{-8}$ mole lead to 17,500 and 15,300 TONs, respectively. Overall, as illustrated in **Figure 3b**, by utilizing $2.3x10^{-8}$ mole of **BDP-Por** the maximum mmol(H_2) g(cat)$^{-1}$ h^{-1} (114) and TONs (17,500) were observed. In **Table S1**, a summary of the photocatalytic H_2 evolution results of **BDP-Por** dyad is provided.

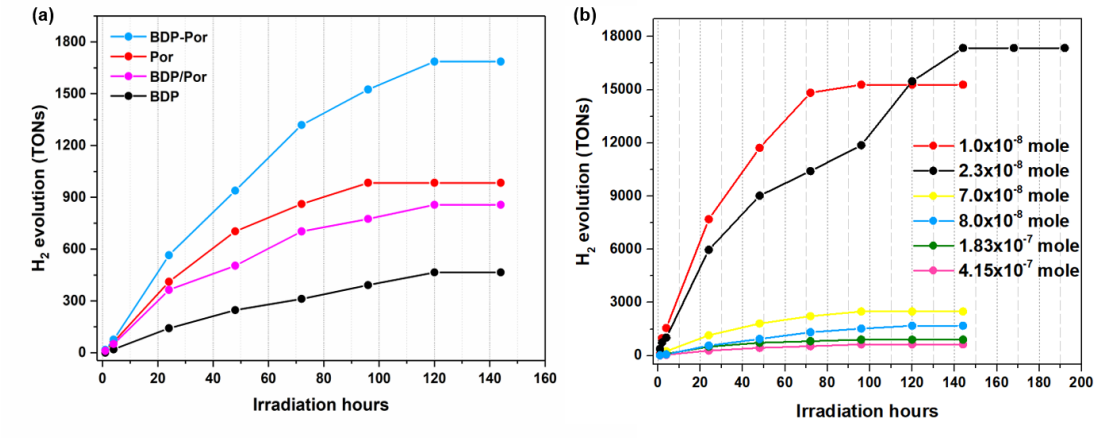

Figure 3. Photocatalytic H_2 evolution plots **(a)**: **BDP** (black), 1:1 mixture of **BDP/Por** (magenta), **Por** (red) and **BDP-Por** dyad (blue), using $8.0x10^{-8}$ mole of each PS **(b)** different amounts of **BDP-Por** dyad onto 10mg of Pt-TiO_2 NPs: $4.15x10^{-7}$ mole (pink line), $1.83x10^{-7}$ mole (green line), $8.0x10^{-8}$ mole (blue line), $7.0x10^{-8}$ mole (yellow line), $2.3x10^{-8}$ mole (black line) and $1.0x10^{-8}$ mole (red line).

In an effort to compare the covalent attachment with the axial coordination, we examined the photocatalytic properties of **BDP(Im)-Por** and related its activity with **BDP-Por**. In addition, with the intention of enhancing the antenna effect, we introduced an additional BODIPY unit (**BDP(Im)**) to **BDP-Por** dyad developing

another hybrid, namely **BDP-Por-BDP(Im)**. In **Figure 4**, the H_2 evolution experiments regarding **Por**, **BDP-Por**, **BDP(Im)-Por** and **BDP-Por-BDP(Im)** are presented. **BDP-Por** exhibited 17,500 TONs, while **BDP(Im)-Por** reached 13,700 TONs. Hence, the covalent approach (**BDP-Por**) was more efficient than the axial one (**BDP(Im)-Por**). As expected, the photocatalytic activity of **BDP-Por-BDP(Im)** was enhanced compared to either **BDP-Por** or **BDP(Im)-Por** due to the supplementary antenna effect and since the additional BODIPY entity acts as an extra light harvester. Overall, **BDP-Por-BDP(Im)** displayed 18,600 TONs and 225 mmol(H_2) g(cat)$^{-1}$ h^{-1}.

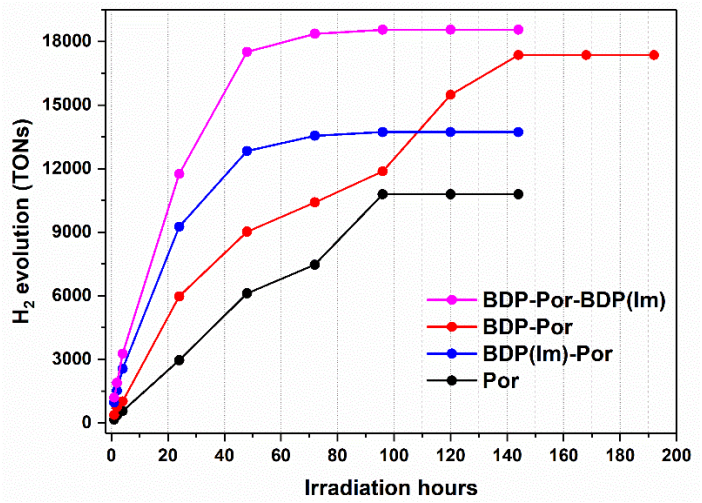

Figure 4. Photocatalytic H_2 production plots of **Por** (black), **BDP(Im)-Por** (blue), **BDP-Por** (red) and **BDP-Por-BDP(Im)** (magenta) using 2.3x10^{-8} mole of the PS onto 10mg of Pt-TiO_2 NPs in 1M AA.

Photoelectrochemical measurements on TiO_2 films

The first and important step, which controls the efficiency of a DSP, is the electron injection into the conduction band of TiO_2 from the photoexcited sensitizer. Accordingly, we have investigated and compared the photoelectrochemical properties of the different molecular components on mesoporous nanocrystalline TiO_2 electrodes to assess the impact of the BODIPY antenna on the photocurrent density (**Figure S8**).

More precisely, the sensitized TiO_2 films were used as working electrodes in three electrode setup in contact with an aqueous electrolyte containing ascorbic acid similarly as that used for the photocatalytic experiments (see experimental part for details). In these conditions, the photoexcited porphyrin decays by electron injection into the TiO_2 film and is regenerated by the AA sacrificial electron donor, while the injected electron is collected by the back electrode contact. First, chopped light linear sweep voltammetry (LSV) between -0.6 V until 0.3 V *vs.* SCE under white light irradiation were conducted (**Figure 5**). The onset potential appears around -0.6 V *vs.* SCE meaning that in these conditions, the electron injection reaction from the porphyrin excited state starts to become thermodynamically favorable and/or the electron transport inside the TiO_2 film outcompetes with charge recombination.

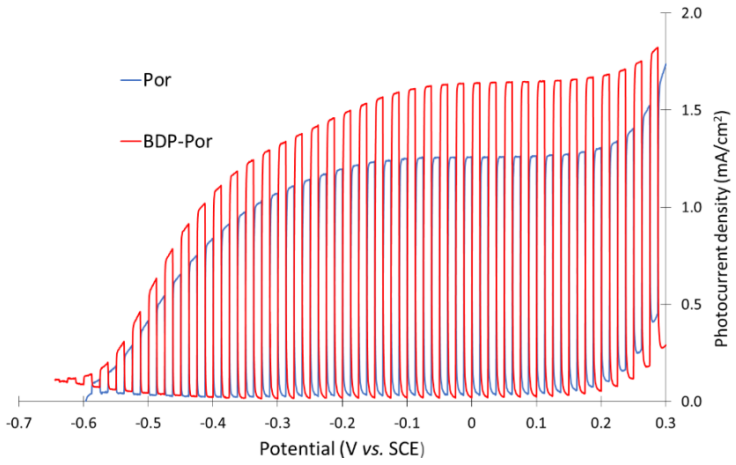

Figure 5. Chopped light linear sweep voltammetry measurements recorded under white light irradiation (350 W/m^2) of the sensitizers chemisorbed on TiO_2 film with the aqueous electrolyte containing [AA] = 1 M, [$LiClO_4$] = 0.1 M at pH = 4. Scan starts from -0.6 V and ends at 0.3 V with scan rate 5 mV/s.

When the applied potential to the photoelectrode is scanned towards more positive values, the photocurrent steadily increases until 0 V *vs.* SCE and remains quite constant. Then, from the potential 0.2 V *vs.* SCE, the photocurrent is

superimposed with the direct electrochemical oxidation of ascorbic acid on the electrode surface. In a second set of experiments, the photocurrent densities of the different systems were recorded at a constant potential of 0 V *vs.* SCE under similar irradiation conditions (**Figure 6** and **S9**). Naturally, when ascorbic acid (AA) is replaced by acetic acid (AcOH), the photoelectrode produces almost no detectable photocurrent under light irradiation proving that the presence of a sacrificial electron donor is mandatory to restore the neutral state of the sensitizer and to observe photoelectrochemical effect (**Figure S10**). Interestingly, in absence of AA in the solution, the voltamogramm displays spikes at the beginning (anodic) and at this end (cathodic) of the light irradiation sequence. The anodic spike is due to charging of the TiO_2 after electron injection, while the cathodic spike observed when the light is turned off is due to the back electron transfer of the electrons in TiO_2 with holes on ZnP^+. Overall, in presence of AA in the electrolyte, it can be observed that the photocurrent density is ranked in the following order: **BDP-Por-BDP(Im)** > **BDP-Por** > **BDP(Im)-Por** > **Por** underscoring that the presence of the BODIPY either covalently linked (**BDP-Por**) or axially assembled (**BDP(Im)-Por** and **BDP-Por-BDP(Im)**) raised the photocurrent density owing to antenna effect coming from energy transfer to the porphyrin. From these values, several conclusions can be drawn. First, the **BDP(Im)** linked to the porphyrin *via* coordination bond is less efficient compare with the covalently linkage in the dyad **BDP-Por**. Second, **BDP(Im)** can, however, enhance the photocurrent density of the dyad **BDP-Por** as it certainly increases the light harvesting efficiency of the photoelectrode. This can be understood as **BDP(Im)** has a red-shifted absorption band relative to that of BODIPY in **BDP-Por** and thus it increases further light collection of **BDP-Por** (**Figure S11**). This assumption is supported by the IPCE spectra of **BDP-Por-BDP(Im)**, which features higher values

around 520-530 nm (**Figure 7**). Interestingly, **BDP(Im)** chemosorbed alone on TiO_2 surface can inject electron into the electrode since a substantial photocurrent density (0.57 mA/cm^2) can be measured, although weaker than **Por** (1.24 mA/cm^2), but with a significant efficiency as compare with **BDP** grafted by carboxylic acid (0.49 mA/cm^2) (**Figure S11**). Accordingly, we cannot rule out that part of the increased photocurrent with **BDP(Im)** can be ascribed to direct electron injection into TiO_2 in addition to energy transfer to the zinc porphyrin.

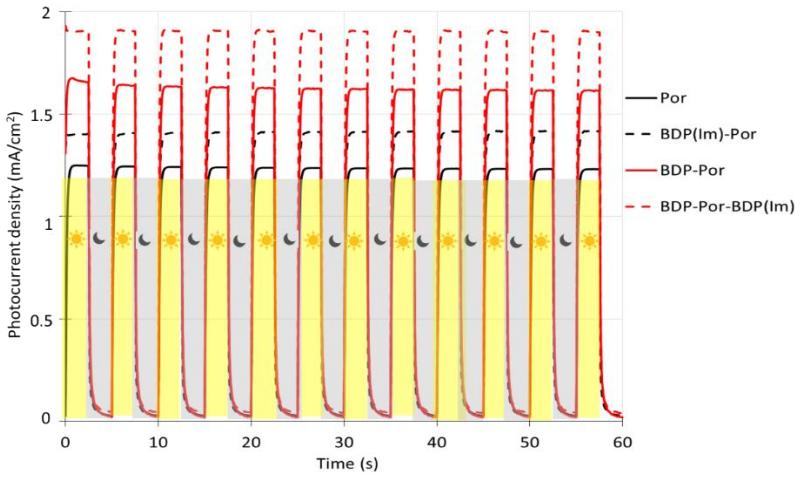

Figure 6. Chopped light voltammetry measurements recorded under white light irradiation (350 W/m^2) of the sensitizers chemisorbed on TiO_2 film with the aqueous electrolyte containing [AA] = 1 M, [$LiClO_4$] = 0.1 M at pH = 4. Applied potential = 0 V *vs.* SCE.

In a following experiment, the Incident Photon-to-electron Conversion Efficiency (IPCE) spectra of the photoelectrodes were recorded under 0 V *vs.* SCE bias (**Figure 7** and **S11**). On one hand, the comparison of the IPCE spectra of **Por** and **BDP-Por** clearly reveals a higher photoresponse of the latter between 450-500 nm, where the BODIPY antenna absorbs, underscoring again the benefit of energy transfer inside the molecule. On the other hand, the comparison of the IPCE spectra of **BDP(Im)-Por** and **BDP-Por** shows that BODIPY unit participates in the photocurrent

production of both compounds, but with a shift of the BODIPY contribution in **BDP(Im)-Por**. We thus concluded that part of the increased efficiency with **BDP(Im)** can be ascribed to direct electron injection into TiO_2 in addition to energy transfer from **BDP(Im)** axially bound by coordination to zinc porphyrin (**Figure S6**). The addition of a supplementary antenna in the dyad **BDP-Por** with **BDP(Im)** also enhances the IPCE values between 450-550 nm because light absorption is increased with this additional chromophore.

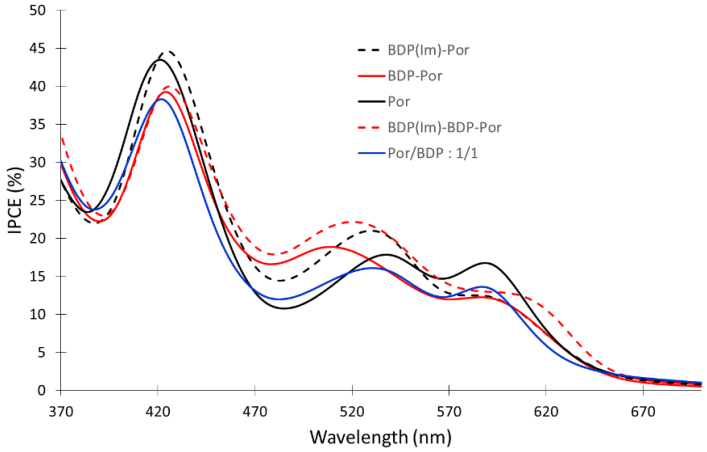

Figure 7. IPCE spectra recorded at applied potential 0 V *vs.* SCE of the sensitizers chemisorbed on TiO_2 film with the aqueous electrolyte containing [AA] = 1 M, [$LiClO_4$] = 0.1 M at pH = 4.

In summary, the photocurrent densities order matches well with that of the H_2 evolution efficiencies of DSPs measured with these different molecular sensitizers, supporting that the role of the BODIPY chromophore is to enhance light absorption of the photocatalytic system and to increase the electron density inside the TiO_2 NPs.

Conclusions.

This work demonstrates that BODIPY-(Zn)Porphyrin dyads **BDP-Por** and **BDP(Im)-Por** are more efficient photosensitizers in photocatalytic H_2 production

compared to their counterparts. We have compared two different approaches regarding the BODIPY-ZnPorphyrin hybrids, namely the covalent attachment *vs.* the axial coordination. Interestingly, the covalent attachment (**BDP-Por**) illustrated greater efficiency (17,500 TONs) compared to the axial coordination (**BDP(Im)-Por**, 13,700 TONs). **BDP-Por** was further functionalized with an additional **BDP(Im)** moiety and the formed hybrid (**BDP-Por-BDP(Im)**) exhibited 18,600 TONs and 225 mmol(H_2) g(cat)$^{-1}$ h^{-1}. Overall, in this study we developed an efficient DSP based on a noble metal-free porphyrin hybrid providing new insights to the wide range research topic of photocatalytic H_2 production. Finally yet importantly, the photocatalytic H_2 evolution results were in perfect agreement with the photoelectrochemical measurements on TiO_2 films revealing that the trend of H_2 production was in line with the photocurrent density values (**Figures 3** and **5**). We illustrated that it is possible to develop highly efficient noble-metal free photosensitizers for photo-induced H_2 evolution based on chromophore dyads that undergo energy transfer process, similar to natural photosynthesis. This work constitutes a proof of principle in the topic of DSPs for H_2 evolution since two well-known chromophores in DSSCs were utilized. Undoubtedly, efficient chromophore polyads that demonstrated enhanced photocurrent features in DSSCs deserve to be studied in DSPs as well. In addition, chromophore polyads with higher or even full spectral coverage will definitely lead to more efficient catalytic results.

Acknowledgements

This research was funded by the General Secretariat for Research and Technology (GSRT) and Hellenic Foundation for Research and Innovation (HFRI; project code: 508). This research has also been co-financed by the European Union and Greek

national funds through the Operational Program Competitiveness, Entrepreneurship, and Innovation, under the call RESEARCH−CREATE−INNOVATE (project code: T1EDK-01504). In addition, this research has been co-financed by the European Union and Greek national funds through the Regional Operational Program "Crete 2014-2020," project code OPS:5029187. Moreover, the European Commission's Seventh Framework Program (FP7/2007-2013) under grant agreement no. 229927 (FP7-REGPOT-2008-1, Project BIO-SOLENUTI) and the Special Research Account of the University of Crete are gratefully acknowledged for the financial support of this research. Région des Pays de la Loire is gratefully acknowledged for the financial support of these researches through the project LUMOMAT.

Supporting information available: Experimental details, photocatalytic H_2 evolution results, additional chopped light voltammetry measurements, IPCE spectra and pictures of the TiO_2 films used for spectroelectrochemistry measurements.

References

(1) Hammarstrom, L.; Hammes-Schiffer, S. Artificial photosynthesis and solar fuels. *Acc. Chem. Res.* **2009,** *42* (12), 1859.

(2) Le Quéré, C.; Jackson, R. B.; Jones, M. W.; Smith, A. J. P.; Abernethy, S.; Andrew, R. M.; De-Gol, A. J.; Willis, D. R.; Shan, Y.; Canadell, J. G.et al. Temporary reduction in daily global CO2 emissions during the COVID-19 forced confinement. *Nat. Clim. Change* **2020,** *10* (7), 647.

(3) Mustafa, A.; Lougou, B. G.; Shuai, Y.; Wang, Z.; Tan, H. Current technology development for CO2 utilization into solar fuels and chemicals: A review. *J. Energy Chem.* **2020,** *49*, 96.

(4) Zhang, B.; Sun, L. Artificial photosynthesis: opportunities and challenges of molecular catalysts. *Chem. Soc. Rev.* **2019,** *48* (7), 2216.

(5) Zhang, J. Z.; Reisner, E. Advancing photosystem II photoelectrochemistry for semi-artificial photosynthesis. *Nat. Rev. Chem.* **2020,** *4* (1), 6.

(6) Smith, P. T.; Nichols, E. M.; Cao, Z.; Chang, C. J. Hybrid Catalysts for Artificial Photosynthesis: Merging Approaches from Molecular, Materials, and Biological Catalysis. *Acc. Chem. Res.* **2020,** *53* (3), 575.

(7) Saraswat, S. K.; Rodene, D. D.; Gupta, R. B. Recent advancements in semiconductor materials for photoelectrochemical water splitting for hydrogen production using visible light. *Renew. Sustain. Energy Rev.* **2018,** *89*, 228.

(8) Li, C.; He, J.; Xiao, Y.; Li, Y.; Delaunay, J.-J. Earth-abundant Cu-based metal oxide photocathodes for photoelectrochemical water splitting. *Energy Environ. Sci.* **2020,** *13* (10), 3269.

(9) Liu, Y.; Huang, D.; Cheng, M.; Liu, Z.; Lai, C.; Zhang, C.; Zhou, C.; Xiong, W.; Qin, L.; Shao, B.et al. Metal sulfide/MOF-based composites as visible-light-driven photocatalysts for enhanced hydrogen production from water splitting. *Coord. Chem. Rev.* **2020,** *409*, 213220.

(10) Hisatomi, T.; Domen, K. Reaction systems for solar hydrogen production via water splitting with particulate semiconductor photocatalysts. *Nat. Catal.* **2019,** *2* (5), 387.

(11) Zhang, J.-H.; Wei, M.-J.; Wei, Z.-W.; Pan, M.; Su, C.-Y. Ultrathin Graphitic Carbon Nitride Nanosheets for Photocatalytic Hydrogen Evolution. *ACS Appl. Nano Mater.* **2020,** *3* (2), 1010.

(12) Christoforidis, K. C.; Fornasiero, P. Photocatalytic Hydrogen Production: A Rift into the Future Energy Supply. *ChemCatChem* **2017,** *9* (9), 1523.

(13) Shi, Y.; Yang, A.-F.; Cao, C.-S.; Zhao, B. Applications of MOFs: Recent advances in photocatalytic hydrogen production from water. *Coord. Chem. Rev.* **2019,** *390*, 50.

(14) Fujishima, A.; Honda, K. Electrochemical Photolysis of Water at a Semiconductor Electrode. *Nature* **1972,** *238* (5358), 37.

(15) Chiarello, G. L.; Dozzi, M. V.; Selli, E. TiO2-based materials for photocatalytic hydrogen production. *J. Energy Chem.* **2017,** *26* (2), 250.

(16) Cai, J.; Shen, J.; Zhang, X.; Ng, Y. H.; Huang, J.; Guo, W.; Lin, C.; Lai, Y. Light-Driven Sustainable Hydrogen Production Utilizing TiO2 Nanostructures: A Review. *Small Methods* **2019,** *3* (1), 1800184.

(17) Kumaravel, V.; Mathew, S.; Bartlett, J.; Pillai, S. C. Photocatalytic hydrogen production using metal doped TiO2: A review of recent advances. *Appl. Catal. B: Environ.* **2019,** *244*, 1021.

(18) Chen, X.; Shen, S.; Guo, L.; Mao, S. S. Semiconductor-based Photocatalytic Hydrogen Generation. *Chem. Rev.* **2010,** *110* (11), 6503.

(19) Manfredi, N.; Monai, M.; Montini, T.; Salamone, M.; Ruffo, R.; Fornasiero, P.; Abbotto, A. Enhanced photocatalytic hydrogen generation using carbazole-based sensitizers. *Sustain. Energy Fuels* **2017,** *1* (4), 694.

(20) Gross, M. A.; Reynal, A.; Durrant, J. R.; Reisner, E. Versatile Photocatalytic Systems for H2 Generation in Water Based on an Efficient DuBois-Type Nickel Catalyst. *J. Am. Chem. Soc.* **2014,** *136* (1), 356.

(21) Yin, M.; Ma, S.; Wu, C.; Fan, Y. A noble-metal-free photocatalytic hydrogen production system based on cobalt(iii) complex and eosin Y-sensitized TiO2. *RSC Adv.* **2015,** *5* (3), 1852.

(22) Warnan, J.; Willkomm, J.; Ng, J. N.; Godin, R.; Prantl, S.; Durrant, J. R.; Reisner, E. Solar H2 evolution in water with modified diketopyrrolopyrrole dyes immobilised on molecular Co and Ni catalyst–TiO2 hybrids. *Chem. Sci.* **2017,** *8* (4), 3070.

(23) Willkomm, J.; Orchard, K. L.; Reynal, A.; Pastor, E.; Durrant, J. R.; Reisner, E. Dye-sensitised semiconductors modified with molecular catalysts for light-driven H2 production. *Chem. Soc. Rev.* **2016,** *45* (1), 9.

(24) Shimidzu, T.; Iyoda, T.; Koide, Y. An advanced visible-light-induced water reduction with dye-sensitized semiconductor powder catalyst. *J. Am. Chem. Soc.* **1985,** *107* (1), 35.

(25) Abe, R.; Hara, K.; Sayama, K.; Domen, K.; Arakawa, H. Steady hydrogen evolution from water on Eosin Y-fixed TiO2 photocatalyst using a silane-coupling reagent under visible light irradiation. *J. Photochem. Photobiol. A* **2000,** *137* (1), 63.

(26) Reginato, G.; Zani, L.; Calamante, M.; Mordini, A.; Dessì, A. Dye-Sensitized Heterogeneous Photocatalysts for Green Redox Reactions. *Eur. J. Inorg. Chem.* **2020,** *2020* (11-12), 899.

(27) Li, G.; Mark, M. F.; Lv, H.; McCamant, D. W.; Eisenberg, R. Rhodamine-Platinum Diimine Dithiolate Complex Dyads as Efficient and Robust Photosensitizers for Light-Driven Aqueous Proton Reduction to Hydrogen. *J. Am. Chem. Soc.* **2018,** *140* (7), 2575.

(28) Ho, P.-Y.; Mark, M. F.; Wang, Y.; Yiu, S.-C.; Yu, W.-H.; Ho, C.-L.; McCamant, D. W.; Eisenberg, R.; Huang, S. Panchromatic Sensitization with ZnII Porphyrin-Based Photosensitizers for Light-Driven Hydrogen Production. *ChemSusChem* **2018,** *11* (15), 2517.

(29) Suryani, O.; Higashino, Y.; Sato, H.; Kubo, Y. Visible-to-Near-Infrared Light-Driven Photocatalytic Hydrogen Production Using Dibenzo-BODIPY and Phenothiazine Conjugate as Organic Photosensitizer. *ACS Appl. Energy Mater.* **2019,** *2* (1), 448.

(30) Sun, Y.; Sun, Y.; Dall'Agnese, C.; Wang, X.-F.; Chen, G.; Kitao, O.; Tamiaki, H.; Sakai, K.; Ikeuchi, T.; Sasaki, S.-i. Dyad Sensitizer of Chlorophyll with Indoline Dye for Panchromatic Photocatalytic Hydrogen Evolution. *ACS Appl. Energy Mater.* **2018,** *1* (6), 2813.

(31) Odobel, F.; Pellegrin, Y.; Warnan, J. Bio-inspired artificial light-harvesting antennas for enhancement of solar energy capture in dye-sensitized solar cells. *Energy Environ. Sci.* **2013,** *6* (7), 2041.

(32) Warnan, J.; Pellegrin, Y.; Blart, E.; Odobel, F. Supramolecular light harvesting antennas to enhance absorption cross-section in dye-sensitized solar cells. *Chem. Commun.* **2012,** *48* (5), 675.

(33) Lee, C. Y.; Hupp, J. T. Dye sensitized solar cells: TiO2 sensitization with a bodipy-porphyrin antenna system. *Langmuir* **2010,** *26* (5), 3760.

(34) Louahem M'Sabah, B.; Boucharef, M.; Warnan, J.; Pellegrin, Y.; Blart, E.; Lucas, B.; Odobel, F.; Bouclé, J. Amplification of light collection in solid-state dye-sensitized solar cells via the antenna effect through supramolecular assembly. *Phys. Chem. Chem. Phys.* **2015,** *17* (15), 9910.

(35) Singh, S. P.; Gayathri, T. Evolution of BODIPY Dyes as Potential Sensitizers for Dye-Sensitized Solar Cells. *Eur. J. Org. Chem.* **2014,** *2014* (22), 4689.

(36) Galateia, Z. E.; Agapi, N.; Vasilis, N.; Sharma, G. D.; Athanassios, C. G. "Scorpion"-shaped mono(carboxy)porphyrin-(BODIPY)2, a novel triazine bridged triad: synthesis, characterization and dye sensitized solar cell (DSSC) applications. *J. Mater. Chem. C* **2015,** *3* (22), 5652.

(37) Andrianov, D. S.; Farré, Y.; Chen, K. J.; Warnan, J.; Planchat, A.; Jacquemin, D.; Cheprakov, A. V.; Odobel, F. Trans-disubstituted benzodiazaporphyrin: A promising hybrid dye between porphyrin and phthalocyanine for application in dye-sensitized solar cells. *J. Photochem. Photobiol. A* **2016,** *330*, 186.

(38) Zani, L.; Melchionna, M.; Montini, T.; Fornasiero, P. Design of dye-sensitized TiO2 materials for photocatalytic hydrogen production: light and shadow. *Journal of Physics: Energy* **2021,** *3* (3), 031001.

(39) Huang, J.-F.; Lei, Y.; Luo, T.; Liu, J.-M. Photocatalytic H2 Production from Water by Metal-free Dye-sensitized TiO2 Semiconductors: The Role and Development Process of Organic Sensitizers. *ChemSusChem* **2020,** *13* (22), 5863.

(40) Tiwari, A.; Krishna, N. V.; Giribabu, L.; Pal, U. Hierarchical Porous TiO2 Embedded Unsymmetrical Zinc–Phthalocyanine Sensitizer for Visible-Light-Induced Photocatalytic H2 Production. *J. Phys. Chem. C* **2017,** *122* (1), 495.

(41) Koposova, E.; Liu, X.; Pendin, A.; Thiele, B.; Shumilova, G.; Ermolenko, Y.; Offenhäusser, A.; Mourzina, Y. Influence of Meso-Substitution of the Porphyrin Ring on Enhanced Hydrogen Evolution in a Photochemical System. *J. Phys. Chem. C* **2016,** *120* (26), 13873.

(42) Gonuguntla, S.; Tiwari, A.; Madanaboina, S.; Lingamallu, G.; Pal, U. Revealing high hydrogen evolution activity in zinc porphyrin sensitized hierarchical porous TiO2 photocatalysts. *Int. J. Hydrog. Energy* **2020,** *45* (13), 7508.

(43) Huang, J.-F.; Lei, Y.; Xiao, L.-M.; Chen, X.-L.; Zhong, Y.-H.; Qin, S.; Liu, J.-M. Photocatalysts for H2 Generation from Starburst Triphenylamine/Carbazole Donor-Based Metal-Free Dyes and Porous Anatase TiO2 Cube. *ChemSusChem* **2020,** *13* (5), 1037.

(44) Bartolini, M.; Gombac, V.; Sinicropi, A.; Reginato, G.; Dessì, A.; Mordini, A.; Filippi, J.; Montini, T.; Calamante, M.; Fornasiero, P.et al. Tuning the Properties of Benzothiadiazole Dyes for Efficient Visible Light-Driven Photocatalytic H2 Production under Different Conditions. *ACS Appl. Energy Mater.* **2020,** *3* (9), 8912.

(45) Ding, H.; Chu, Y.; Xu, M.; Zhang, S.; Ye, H.; Hu, Y.; Hua, J. Effect of π-bridge groups based on indeno[1,2-b]thiophene D–A–π–A sensitizers on the

performance of dye-sensitized solar cells and photocatalytic hydrogen evolution. *J. Mater. Chem. C* **2020,** *8* (42), 14864.

(46) Ding, H.; Xu, M.; Zhang, S.; Yu, F.; Kong, K.; Shen, Z.; Hua, J. Organic blue-colored D-A-π-A dye-sensitized TiO2 for efficient and stable photocatalytic hydrogen evolution under visible/near-infrared-light irradiation. *Renew. Energy* **2020,** *155*, 1051.

(47) Panda, M. K.; Lazarides, T.; Charalambidis, G.; Nikolaou, V.; Coutsolelos, A. G. Five-Coordinate Indium(III) Porphyrins with Hydroxy and Carboxy BODIPY as Axial Ligands: Synthesis, Characterization and Photophysical Studies. *Eur. J. Inorg. Chem.* **2015,** *2015* (3), 468.

(48) Weber, M. D.; Nikolaou, V.; Wittmann, J. E.; Nikolaou, A.; Angaridis, P. A.; Charalambidis, G.; Stangel, C.; Kahnt, A.; Coutsolelos, A. G.; Costa, R. D. Benefits of using BODIPY–porphyrin dyads for developing deep-red lighting sources. *Chem. Commun.* **2016,** *52* (8), 1602.

(49) S. Lindsey, J.; Prathapan, S.; E. Johnson, T.; W. Wagner, R. Porphyrin building blocks for modular construction of bioorganic model systems. *Tetrahedron* **1994,** *50* (30), 8941.

(50) Weber, M. D.; Nikolaou, V.; Wittmann, J. E.; Nikolaou, A.; Angaridis, P. A.; Charalambidis, G.; Stangel, C.; Kahnt, A.; Coutsolelos, A. G.; Costa, R. D. Benefits of using BODIPY–porphyrin dyads for developing deep-red lighting sources. *Chemical Communications* **2016,** *52* (8), 1602.

(51) Mathew, S.; Yella, A.; Gao, P.; Humphry-Baker, R.; Curchod, B. F.; Ashari-Astani, N.; Tavernelli, I.; Rothlisberger, U.; Nazeeruddin, M. K.; Gratzel, M. Dye-sensitized solar cells with 13% efficiency achieved through the molecular engineering of porphyrin sensitizers. *Nature Chem.* **2014,** *6* (3), 242.

(52) Ma, T.; Inoue, K.; Noma, H.; Yao, K.; Abe, E. Effect of functional group on photochemical properties and photosensitization of TiO2 electrode sensitized by porphyrin derivatives. *J. Photochem. Photobiol. A* **2002,** *152* (1-3), 207.

(53) Lee, C. W.; Lu, H. P.; Lan, C. M.; Huang, Y. L.; Liang, Y. R.; Yen, W. N.; Liu, Y. C.; Lin, Y. S.; Diau, E. W.; Yeh, C. Y. Novel zinc porphyrin sensitizers for dye-sensitized solar cells: synthesis and spectral, electrochemical, and photovoltaic properties. *Chem. Eur. J.* **2009,** *15* (6), 1403.

(54) Ma, T.; Inoue, K.; Yao, K.; Noma, H.; Shuji, T.; Abe, E.; Yu, J.; Wang, X.; Zhang, B. Photoelectrochemical properties of TiO2 electrodes sensitized by porphyrin derivatives with different numbers of carboxyl groups. *J. Electroanal. Chem.* **2002,** *537* (1-2), 31.

(55) Kobuke, Y. Porphyrin Supramolecules by Self-Complementary Coordination. *Struct. Bonding* **2006,** *121*, 49.

(56) Hu, Q. Q.; Zhu, Y. Z.; Zhang, S. C.; Tong, Y. Z.; Zheng, J. Y. meso-2'-Linked porphyrin-BODIPY hybrids: synthesis and efficient excitation energy transfer. *Dalton Trans.* **2015,** *44* (35), 15523.

(57) Leonardi, M. J.; Topka, M. R.; Dinolfo, P. H. Efficient Forster resonance energy transfer in 1,2,3-triazole linked BODIPY-Zn(II) meso-

tetraphenylporphyrin donor-acceptor arrays. *Inorg. Chem.* **2012,** *51* (24), 13114.

(58) Lazarides, T.; Charalambidis, G.; Vuillamy, A.; Reglier, M.; Klontzas, E.; Froudakis, G.; Kuhri, S.; Guldi, D. M.; Coutsolelos, A. G. Promising fast energy transfer system via an easy synthesis: Bodipy-porphyrin dyads connected via a cyanuric chloride bridge, their synthesis, and electrochemical and photophysical investigations. *Inorg. Chem.* **2011,** *50* (18), 8926.

(59) Warnan, J.; Buchet, F.; Pellegrin, Y.; Blart, E.; Odobel, F. Panchromatic trichromophoric sensitizer for dye-sensitized solar cells using antenna effect. *Org. Lett.* **2011,** *13* (15), 3944.